International Journal on
"Technical and Physical Problems of Engineering"
(IJTPE)
Published by International Organization on TPE (IOTPE)

ISSN 2077-3528
IJTPE Journal
www.iotpe.com
ijtpe@iotpe.com

June 2010	Issue 3	Volume 2	Number 2	Pages 45-51

ROBUST LOOP-SHAPING BASED POD CONTROLLER DESIGN FOR UPFC

H. Shayeghi [1] H.A. Shayanfar [2] F. Shalchi [2]

1 Technical Engineering Department, University of Mohaghegh Ardabili, Ardabil, Iran, hshayeghi@gmail.com
2 Center of Excellence for Power Automation and Operation, Electrical Engineering Department, Iran University of Science and Technology, Tehran, Iran, hashayanfar@yahoo.com

Abstract- Power systems such as the other industrial plants contain different kinds of uncertainties which should be considered in controller design procedure. For this reason, the idea of robust loop-shaping control was used for designing of UPFC Power Oscillation Damping (POD) controller. This approach provides a robust controller that performs satisfactorily for a wide range of operating conditions and under certain degree of uncertainties. The effectiveness of the proposed control strategy was evaluated under operating conditions for damping low frequency oscillations in comparison with the classical controller to demonstrate its robust performance through time-domain simulation.

Keywords: UPFC, Loop-Shaping Controller, Robust Control, FACTS, Power System Stability and Control.

I. INTRODUCTION

As power demand grows rapidly and expansion in transmission and generation is restricted with the limited availability of resources and the strict environmental constraints, power systems are today much more loaded than before. In addition, the modern power system tends to be interconnected to obtain the most economic benefits. However, interconnection between remotely located power system give rises to occur low frequency oscillations on heavily loaded tie-lines especially after large or small disturbance in the range of 0.1-3.0 Hz. This causes the power systems to be operated near their stability limits. On the other hand, these oscillations constraints the capability of power transmission, threatens system security and damages the efficient operation of the power system. Thus, mitigation of low-frequency oscillations is necessary for secure operation of power systems. In recent years, the fast progress in the field of power electronics has opened new opportunities for the power industry via utilization of the controllable FACTS devices such as UPFC, TCSC and SVC which offer an alternative means to mitigate power system oscillations [1]. Because of the extremely fast control action associated with FACTS-device operations, they have been very promising candidates for mitigation power system oscillation in addition to improve power system steady-state performance [2-3]. UPFC is regarded as one of the most versatile devices in the FACTS device family [4-5], has the capabilities of control power flow in the transmission line, improving the transient stability, mitigation system oscillation and providing voltage support. The application of the UPFC to the modern power system can therefore lead to more flexible, secure and economic operation [6].

An industrial process, such as a power system, contains different kinds of uncertainties due to changes in system parameters and characteristics, loads variation and errors in the modeling. As a result, a fixed parameter controller based on the classical control theory such as PI or lead-lag controller [3, 7-9] is not certainly suitable for a UPFC control method. Thus, some authors have suggested fuzzy logic controllers [10] and neural networks method [11] to deal with system parameters changes for enhance system damping performance. However, the parameters adjustments of these controllers need some trial and error. On the other hand, several authors have been applied robust control methodologies [12-13] to cope with system uncertainties for mitigation low frequency oscillation using UPFC. The requirement for the power system damping controllers is to ensure that the oscillations have enough damping ratio under all possible operating conditions. In practice, it is required that the UPFC damping controller should have the ability to perform satisfactorily under a wide range of operating conditions, and in the presence of uncertainties, i.e. disturbances and errors due to monitoring instruments. Based on this framework, a robust Power Oscillation Damping (POD) controller is designed for satisfying UPFC performance based on loop-shaping technique to mitigate low frequency oscillations. This approach provides a robust controller that performs satisfactorily for a wide range of operating conditions and under certain degree of uncertainties.

The proposed control strategy is compared with the classical PID controllers to illustrate its robust performance under different operation conditions for damping low frequency oscillation and load disturbances. The performance of the proposed control scheme has fulfilled the robust stability and robust performance criteria. Furthermore, time-domain simulation has proved that using the proposed controller, the power oscillation damping behavior is also satisfactory under large disturbances.

II. SYSTEM MODEL

Figure 1 shows a SMIB system equipped with a UPFC. The UPFC consists of an excitation transformer (ET), a boosting transformer (BT), two three-phase GTO based voltage source converters (VSCs), and a DC link capacitors. The four input control signals to the UPFC are m_E, m_B, δ_E, and δ_B, where, m_E is the excitation amplitude modulation ratio, m_B is the boosting amplitude modulation ratio, δ_E is the excitation phase angle and δ_B is the boosting phase angle.

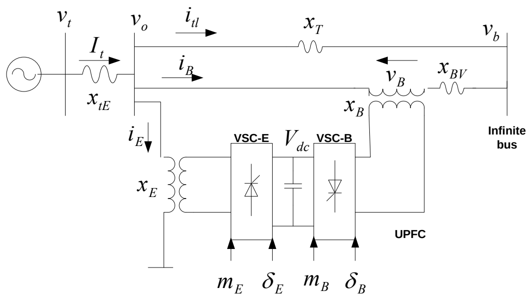

Figure 1. SMIB power system equipped with UPFC

The power system linearized model is described as the following. A linear dynamic model is obtained by linearising the nonlinear model as given in [14] around an operating condition. The linearized model of power system as shown in Figure 1 is given as follows:

$$\Delta\dot{\delta} = \omega_0 \Delta\omega \tag{1}$$

$$\Delta\dot{\omega} = (-\Delta P_e - D\Delta\omega)/M \tag{2}$$

$$\Delta \dot{E}_q^{/} = (-\Delta E_q + \Delta E_{fd})/T_{do}^{/} s \tag{3}$$

$$\Delta \dot{E}_{fd} = -\frac{1}{T_A}\Delta E_{fd} - \frac{K_A}{T_A}\Delta V \tag{4}$$

$$\Delta \dot{v}_{dc} = K_7 \Delta\delta + K_8 \Delta E_q^{/} - K_9 \Delta v_{dc} + K_{ce}\Delta m_E + K_{c\delta e}\Delta\delta_E + K_{cb}\Delta m_B + K_{c\delta b}\Delta\delta_B \tag{5}$$

where,

$$\Delta P_e = K_1 \Delta\delta + K_2 \Delta E_q^{/} + K_{pd}\Delta v_{dc} + K_{pe}\Delta m_E + K_{p\delta e}\Delta\delta_E + K_{pb}\Delta m_B + K_{p\delta b}\Delta\delta_B$$

$$\Delta E_q^{/} = K_4 \Delta\delta + K_3 \Delta E_q^{/} + K_{qd}\Delta v_{dc} + K_{qe}\Delta m_E + K_{q\delta e}\Delta\delta_E + K_{qb}\Delta m_B + K_{q\delta b}\Delta\delta_B$$

$$\Delta V_t = K_5 \Delta\delta + K_6 \Delta E_q^{/} + K_{vd}\Delta v_{dc} + K_{ve}\Delta m_E + K_{v\delta e}\Delta\delta_E + K_{vb}\Delta m_B + K_{v\delta b}\Delta\delta_B$$

K_1, K_2, K_9, K_{pu} ,K_{qu} and K_{vu} are linearization constants. The state-space model of power system is given by:

$$\dot{x} = Ax + Bu \tag{6}$$

where, the state vector x, control vector u, A and B are:

$$x = [\Delta\delta \quad \Delta\omega \quad \Delta E_q' \quad \Delta E_{fd} \quad \Delta v_{dc}]$$

$$u = [\Delta m_E \quad \Delta\delta_E \quad \Delta m_B \quad \Delta\delta_B]^T$$

The block diagram of the linearized dynamic model of the SMIB power system with UPFC is shown in Figure 2.

$$A = \begin{bmatrix} 0 & w_0 & 0 & 0 & 0 \\ -\frac{K_1}{M} & 0 & -\frac{K_2}{M} & 0 & -\frac{K_{pd}}{M} \\ -\frac{K_4}{T_{do}^{/}} & 0 & -\frac{K_3}{T_{do}^{/}} & \frac{1}{T_{do}^{/}} & -\frac{K_{qd}}{T_{do}^{/}} \\ -\frac{K_A K_5}{T_A} & 0 & -\frac{K_A K_6}{T_A} & -\frac{1}{T_A} & -\frac{K_A K_{vd}}{T_A} \\ K_7 & 0 & K_8 & 0 & -K_9 \end{bmatrix}$$

$$B = \begin{bmatrix} 0 & 0 & 0 & 0 \\ -\frac{K_{pe}}{M} & -\frac{K_{p\delta e}}{M} & -\frac{K_{pb}}{M} & -\frac{K_{p\delta b}}{M} \\ -\frac{K_{qe}}{T_{do}^{/}} & -\frac{K_{q\delta e}}{T_{do}^{/}} & -\frac{K_{qb}}{T_{do}^{/}} & -\frac{K_{q\delta b}}{T_{do}^{/}} \\ -\frac{K_A K_{vc}}{T_A} & -\frac{K_A K_{v\delta e}}{T_A} & -\frac{K_A K_{vb}}{T_A} & -\frac{K_A K_{v\delta b}}{T_A} \\ K_{ce} & K_{c\delta e} & K_{cb} & K_{c\delta b} \end{bmatrix}$$

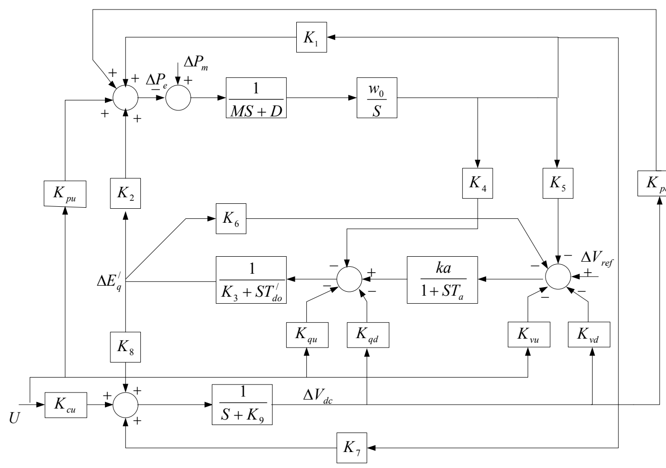

Figure 2. Modified Heffron-Phillips transfer function model

III. UPFC CONTROLLER

The main goals of the UPFC controller design are: power system oscillation damping, DC voltage regulator and power flow controller. A damping controller is provided to improve the damping of power system oscillations. This controller may be considered as a lead-lag compensator. The four control parameters of the UPFC (m_B, m_E, δ_B and δ_E) can be modulated in order to produce the damping torque. In this study, δ_E is modulated in order to damping controller design. The speed deviation $\Delta\omega$ is considered as the input to the damping controllers. The structure of UPFC based damping controller is shown in Figure 3. It consists of gain, signal washout and phase compensator blocks. The parameters of the damping controller using the phase compensation technique for the nominal operating condition as given in Appendix are obtained as follows:

$$\text{Damping Controller} = \frac{536.0145s\ (s+3.656)}{(s+0.1)\ (s+4.5)}$$

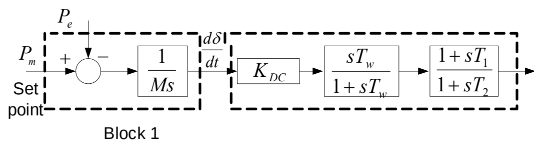

Figure 3. Transfer function block diagram of UPFC based damping controller

The Power flow and DC voltage regulator controller is as the following. The UPFC is installed in one of the two line of the SMIB system. Figure 4 shows the transfer function of the power flow controller. The power flow controller regulates the power flow on this line. k_{pp} and k_{pi} are the proportional and integral gain setting of the power flow controller.

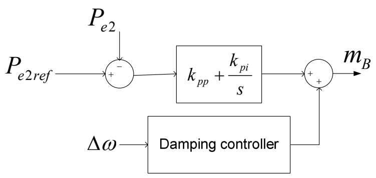

Figure 4. Power flow controller with damping controller

The real power output of the shunt converter must be equal to the real power input of the series converter or vice versa. In order to maintain the power balance between the two converters, a DC voltage regulator is incorporated. DC voltage is regulated by modulating the phase angle of the shunt converter voltage. A P-I type DC-voltage regulator is considered (Figure 5). k_{dp} and k_{di} are the proportional and integral gain settings of the DC regulator.

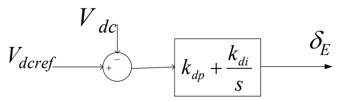

Figure 5. DC voltage regulator

IV. ROBUST LOOP-SHAPING BASED UPFC POD CONTROLLER SYNTHESIS

We now proceed to design a power flow and DC voltage robust controller using the robust loop-shaping technique. The power system with UPFC robust loop-shaping controller is shown in Fig. 6, where G_p represents the power system model and H_p represents the UPFC robust loop-shaping POD controller, respectively. The controller design procedure is based on the method presented by Glover and McFarlane [15]. In order to optimize closed loop performance requirements, pre- and post-compensation of the plant model G_p should be first carried out. The objective of this process is to shape the open loop singular values of G_p prior to the robust controller design procedure.

$$G_{ps} = W_{post}.G_p.W_{pre} \tag{7}$$

where, G_{ps} represents shaped plant and W_{pre} and W_{post} are pre- and post-compensation function, respectively. W_{post} is chosen as a constant and W_{pre} contains dynamic shaping. The closed loop system is shown in Figure 6.

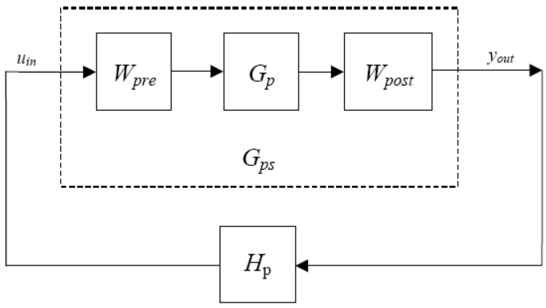

Figure 6. Loop-shaping of the plant

The above-mentioned shaped plant G_{ps} with feedback control and uncertainties can be expressed in form of coprime factors of the plant shown in Figure 7 [15].

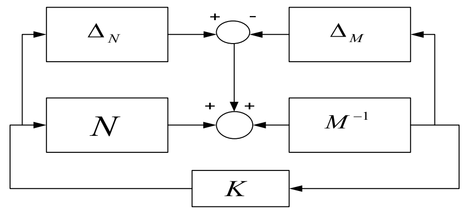

Figure 7. Plant with controller and coprime factor uncertainty

In Figure 7, K represents the UPFC robust loop-shaping damping controller that stabilizes the system G_{ps}. The stabilization of a plant G_{ps} is considered, that has a normalized left coprime factorization as follows:

$$G = M^{-1} \tag{8}$$

A perturbed plant model G_{pr} can then de written as:

$$G_{pr} = \left(M + \Delta_M\right)^{-1} + \left(N + \Delta_N\right) \tag{9}$$

where, Δ_M and Δ_N represent the uncertainty in the nominal plant model G_p. The objective of robust stabilization is to stabilize a family of perturbed plants defined by:

$$G_{pr} = \left\{\left(M + \Delta_M\right)^{-1} + \left(N + \Delta_N\right) : \left\|\left[\Delta_N \quad \Delta_M\right]\right\|_\infty \prec \varepsilon\right\} \tag{10}$$

where, $\varepsilon > 0$ is the stability margin for the perturbed feedback system of Figure 7. If and only if, the nominal feedback system is stable and:

$$\gamma \overset{\Delta}{=} \left\|\begin{bmatrix} K \\ I \end{bmatrix}\left(I - GK\right)^{-1} M^{-1}\right\|_\infty \le \frac{1}{\varepsilon} \tag{11}$$

The lowest achievable value of γ and corresponding maximum stability margin ε are given by:

$$\gamma_{\min} = \varepsilon_{MAX}^{-1} = \left\{1 - \left\|\left[N \quad M\right]\right\|_H^Z\right\}^{1/2} = \left(1 + \rho\left(X_z\right)\right)^{1/2} \tag{12}$$

where $\|.\|_H$ denotes the Hankel norm, ρ denotes radius (maximum eigenvalue), and for minimal state space realization (A, B, C, D) of G, Z and X are the unique positive definite solution of the algebraic Riccati equations:

$$Z : \left(A - BS^{-1}D^T C\right)Z + Z\left(A - BS^{-1}D^T C\right) \\ -ZC^T R^{-1} CZ + BS^{-1}B^T = 0 \tag{13}$$

$$X:\left(A-BS^{-1}D^{T}C\right)X+X\left(A-BS^{-1}D^{T}C\right) \quad (14)$$
$$-XBS^{-1}B^{T}X+C^{T}R^{-1}C=0$$

where $R=I+DD^{T}$ and $S=I+D^{T}D$.

A controller, which guarantees that:

$$\left\| \begin{bmatrix} K \\ I \end{bmatrix} \left(I-GK\right)^{-1} M^{-1} \right\|_{\infty} \le \gamma$$

For a specified $\gamma > \gamma_{\min}$ is given by:

$$K \triangleq \begin{bmatrix} A+BF+\gamma^{2}\left(L^{T}\right)^{-1}ZC^{T}\left(C+DF\right) & \gamma^{2}\left(L^{T}\right)^{-1}ZC^{T} \\ B^{T}X & -D^{T} \end{bmatrix} \quad (15)$$

where, $F=-S^{-1}\left(D^{T}C+B^{T}X\right)$ and $L=\left(1-\gamma^{2}\right)I+ZX$.

It is important to emphasizes that, since $\gamma_{\min}$ is computed from (12) and the explicit solution has been derived by solving just two Riccati equation and the γ iteration needed to solve them, the general H_{∞} problem has been avoided [15]. The controller design procedure as given in [16].

According to the synthesis methodology described in pervious section, our next task is to design. First, the singular values of the open loop are calculated and plotted. We want to maximize the open-loop gain to get the best possible performance, but for robustness, we need to drop the gain below 0dB where the model accuracy is poor and high gain might cause instabilities. This requires a good model where performance is needed (typically at low frequencies), and sufficient roll-off at higher frequencies where the model is often poor. The frequency W_{C}, where the gain crosses the 0dB line, is called the crossover frequency and marks the transition between performance and robustness requirements. After trial and error, target loop shape for power flow and Dc voltage controllers is chosen:

$$G_{d-pf}=15.5\cdot\frac{(s+0.61)}{s(s+1.8)(s+10)}, \quad G_{d-dc}=15\frac{(s+2)}{s(s+5)}$$

The variable $(\gamma_{\min})$ is the inverse of the magnitude of coprime uncertainty, which can be tolerated before getting instability. $\gamma_{\min}\ge 1$ Should be small as possible, and usually requires that $\gamma_{\min}$ is less than a value of 4 [2, 3, 5]. By applying this, $\gamma_{\min}=1.3104$ for power flow controller and $\gamma_{\min}=1.3236$ for the DC voltage regulator are obtained. In order to show influence of H_{∞} loop-shaping method, the proposed method is compare to classical method. In classic method, the parameters of the power-flow controller (k_{pp} and k_{pi}) are optimized using genetic algorithm [17]. Optimum values of the proportional and integral gain settings of the power-flow controller are obtained as $k_{pp}=2$ and $k_{pi}=10$.

The parameters of DC voltage regulator are now optimized using genetic algorithm. When the parameter of power flow controller are set at their optimum values. The optimum gain setting of P-I type DC voltage regulator are $k_{dp}=0.25$ and $k_{di}=0.35$ and damping controller m_{B} was designed according to phase compensation method [14]. Power flow controller damping with damping ratio of 0.5,

$$\text{Damping Controller}=\frac{536.0145\, s\,\left(s+3.656\right)}{\left(s+0.1\right)\left(s+4.5\right)}$$

Now the order of K is reduced to derive reduced controllers as follows:

$$K_{pf}=-0.0191\frac{(s-1067)(s+0.247)(s+0.1468)(s^{2}0.948s+1.33)}{s(s+15.31)(s^{2}+0.3563s+0.03326)(s^{2}+0.7618s+1.272)}$$

$$K_{dc}=84056.5449\frac{(s+17.44)(s+0.559)(s^{2}+1.72s+1.536)}{s(s+4126)(s+40.14)(s+8.87)(s+0.6215)}$$

V. SIMULATION RESULTS

In order to examine the robustness of the robust UPFC power-flow and DC voltage regulator controller in the presence of wide variation in loading condition, the system load is varied over a wide range. The performance of the proposed robust and classical UPFC controllers with the damping controller m_{B} following a 10% step change in reference point of the power line 2 and mechanical power is shown in Figures 8 to 10 for power flow, DC voltage and frequency deviations. The loading condition and system parameters are given in Appendix.

From the simulation results under different operating conditions, it can be seen that the proposed robust loop-shaping UPFC controllers is very effective, achieve good robust performance and compared to classical controller have the best ability to damp power system low frequency oscillations.

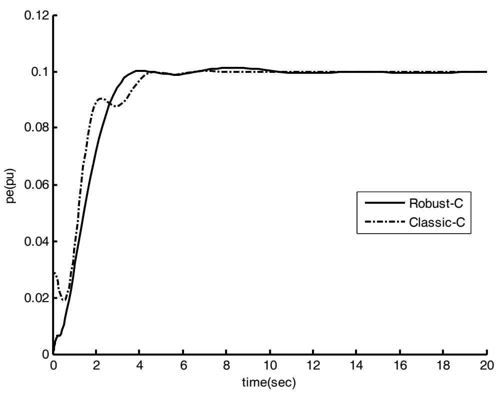

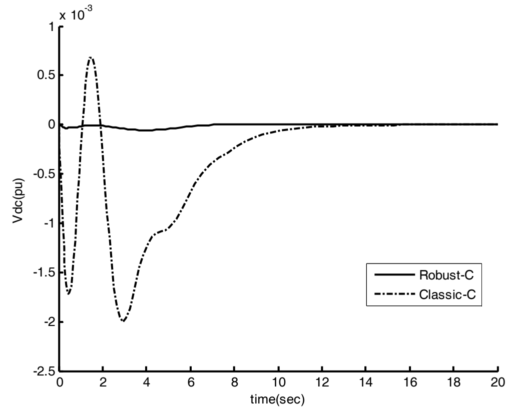

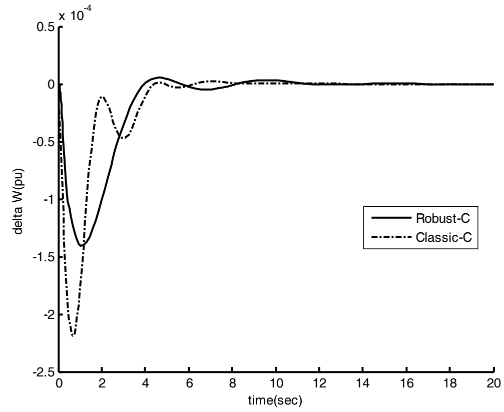

Figure 8. Power system response for operation point 1 under ΔP_{e2fer}=0.1 pu

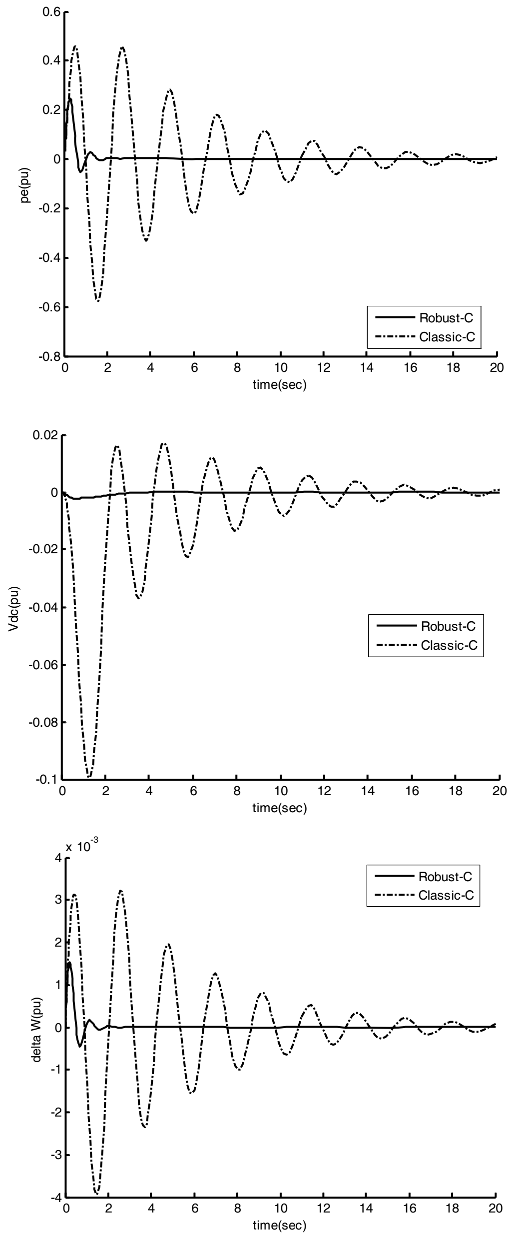

Fig. 9. Power system response for operation point 2 under ΔT_m =0.1 pu

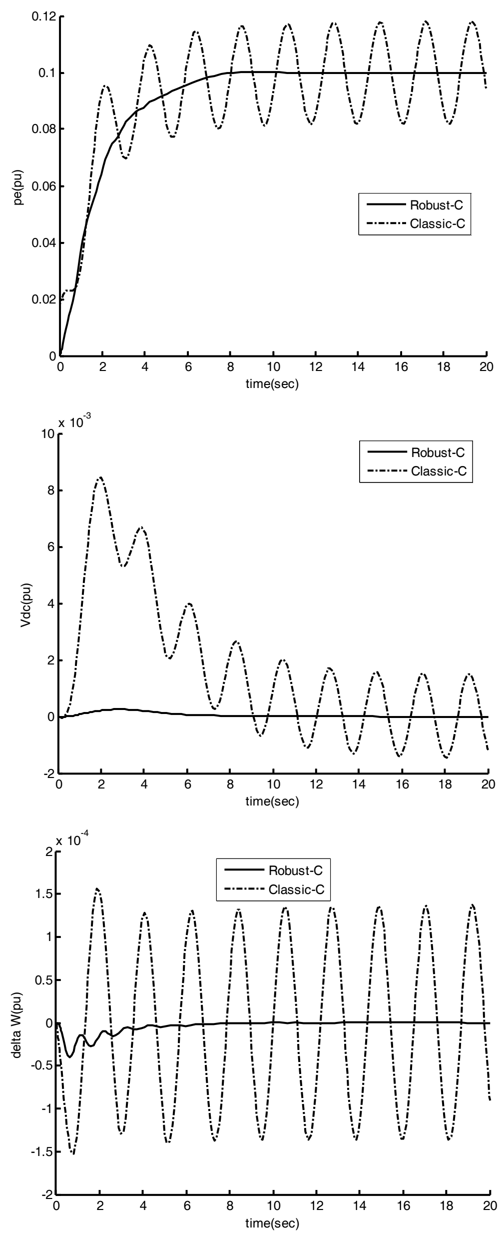

Figure 10. Power system response for operation point 3 under ΔP_{e2fer}=0.1 pu

VI. CONCLUSIONS

In this paper, a robust controller for UPFC based on loop-shaping technique is proposed to mitigate low frequency oscillations. The motivation of using this control strategy is flexibility of the synthesis procedure for modeling uncertainty, direct formulation of performance objectives and practical constraints. The time domain simulation results show that it achieve good performance for damping low frequency oscillations and improves the transient stability under different operating conditions and disturbances. Also, it is superior to the classical controllers. Thus, it is recommended to generate good quality and reliable electric energy in the power systems.

APPENDICES

The nominal parameters and operating condition of the system are listed in Tables 1 and 2.

Table 1. System parameters

Generator	$M = 8$ MJ/MVA	$T'_{do} = 5.044$ s	$X_d = 1$ pu
	$X_q = 0.6$p.u	$X'_d = 0.3$pu	$D = 0$
Excitation system		$K_a = 10$	$T_a = 0.05$ s
Transformers		$X_{tE} = 0.1$ pu	$X_E = 0.1$ pu
		$X_B = 0.1$ pu	
Transmission line		$X_{T1} = 1$ pu	$X_{T2} = 1.3$ pu
Operating condition		$P = 0.8$ pu	$Q = 0.15$ pu
		$V_t = 1.032$ pu	
DC link parameter		$V_{DC} = 2$ pu	$C_{DC} = 3$ pu
UPFC parameter		$m_B = 0.104$	$\delta_B = -55.87^\circ$
		$\delta_E = 26.9^\circ$	$m_E = 1.0233$

Table 2. Operating conditions

1	$P = 0.80$	$Q = 0.15$	$V_t = 1.032$
2	$P = 1.00$	$Q = 0.20$	$V_t = 1.032$
3	$P = 1.125$	$Q = 0.285$	$V_t = 1.032$

REFERENCES

[1] P.L. So and T. Yu, “Coordination of TCSC and SVC for Inter-Area Stability Enhancement”, IEEE Transactions on Power Delivery, Vol. 9, No. 1, 2000.

[2] A.T. Al-Awami, Y.L Abdel-Magid and M.A. Abido, “A Particle-Swarm-Based Approach of Power System Stability Enhancement with Unified Power Flow Controller”, Electrical Power and Energy Systems, Vol. 29, pp. 251-259, 2007.

[3] K.R. Padiyar and H.V. Saikumar, “Coordinated Design and Performance Evaluation of UPFC Supplementary Modulation Controllers, “Electrical Power and Energy Systems, Vol. 27, pp. 101-111, 2005.

[4] L. Gyugyi, “Unified Power-Flow Control Concept for Flexible AC Transmission Systems”, IEE Proceedings on Generation, Transmission & Distribution, Vol. 139, No. 4, pp. 323-31, 1992.

[5] N.G. Hingorani and L. Gyugyi, “Understanding FACTS”, IEEE Press, New York, 2000.

[6] Z. Huang and Y. Ni, “Application of Unified Power Flow Controller in Interconnected Power Systems Modeling, Interface, Control Strategy and Case Study”, IEEE Transactions on Power Systems, Vol. 15, No. 2, pp. 817-24, 2000.

[7] P.C. Stefanov, A.M. Stankovic, “Modeling of UPFC Operation Under Unbalanced Conditions with Dynamic Phasors”, IEEE Transactions on Power Systems, Vol. 17, No. 2, pp. 395-403, 2002.

[8] N. Tambey and M.L. Kothari, “Damping of Power System Oscillations with Unified Power Flow Controller (UPFC)”, IEE Proceedings on Generation, Transmission & Distribution, Vol. 150, No. 2, pp. 129-40, 2003.

[9] M.M. Farsangi, Y.H. Son and K.Y. Lee, “Choice of FACTS Device Control Inputs for Damping Interarea Oscillations”, IEEE Transactions on Power Systems, Vol. 19, No. 2, pp. 1135-43, 2004.

[10] S. Mishra, P.K. Dash and G. Panda, “TS-Fuzzy Controller for UPFC in a Multi-Machine System”, IEE Proceedings on Generation, Transmission & Distribution, Vol. 147, No. 1, pp. 15-22, 2000.

[11] P.K. Dash, S. Mishra and G. Panda, “A Radial Basis Function Neural Network Controller for UPFC”, IEEE Transactions on Power Systems, Vol. 15, No. 4, pp. 1293-9, 2000.

[12] M. Vilathgamuwa, X. Zhu and S.S. Choi, “A Robust Control Method to Improve the Performance of a Unified Power Flow Controller”, Electric Power System Research, Vol. 55, pp. 103-11, 2000.

[13] B.C. Pal, “Robust Damping of Interarea Oscillations with Unified Power Flow Controller”, IEE Proceedings on Generation, Transmission & Distribution, Vol. 149, No. 6, pp.733-8, 2002.

[14] H.F. Wang, “Application of Modeling UPFC into Multi-Machine Power Systems, IEE Proceedings on Generation, Transmission & Distribution, Vol. 146, No. 3, pp. 306-121, 1999.

[15] K.M. Zhou and J.C. Doyle, “Essentials of Robust Control”, Prentice Hall, September 1997.

[16] R.Y. Chiang and M.G. Safonov, “Matlab Robust Control Toolbox - User’s Guide”, The MathWorks Inc., 2010.

[17] H. Shayeghi, A. Jalili and H.A. Shayanfar, “Robust Modified GA Based Multi-Stage Fuzzy LFC”, Energy Conversion and Management, Vol. 48, pp. 1656-1670, 2007.

BIOGRAPHIES

Hossein Shayeghi received the B.S. and M.S.E. degrees in Electrical and Control Engineering in 1996 and 1998, respectively. He received his Ph.D. degree in Electrical Engineering from Iran University of Science and Technology, Tehran, Iran in 2006. Currently, he is an Assistance Professor in Technical Engineering Department of University of Mohaghegh Ardebili, Ardebil, Iran. His research interests are in the Application of Robust Control, Artificial Intelligence to Power System Control Design, Operation and Planning and Power System Restructuring. He is a member of Iranian Association of Electrical and Electronic Engineers and IEEE.

Heidar Ali Shayanfar received the B.Sc. and M.S.E. degrees in Electrical Engineering in 1973 and 1979, respectively. He received his Ph.D. degree in Electrical Engineering from Michigan State University, U.S.A., in 1981. Currently, he is a Full Professor in Electrical Engineering Department of Electrical Engineering, Iran University of Science and Technology, Tehran, Iran. His research interests are in the Application of Artificial Intelligence to Power System Control Design, Dynamic Load Modeling, Power System Observability Studies, Voltage Collapse, Congestion Management in a Restructured Power System, Reliability Improvement in Distribution Systems and Reactive Pricing in Deregulated Power Systems. He is a member of Iranian Association of Electrical and Electronic Engineers and IEEE.

Farshid Shalchi received the B.S. and M.S. degrees in Electrical Engineering from Islamic Azad University, Ardabil Branch and Iran University of Science and Technology, Tehran, Iran in 2004 and 2010, respectively. His areas of interest in research are Application of Robust Control to Power System Control.